

Electronic Supplementary Information

Etienne de Chambost et al.

1 Database of the 183 case studies

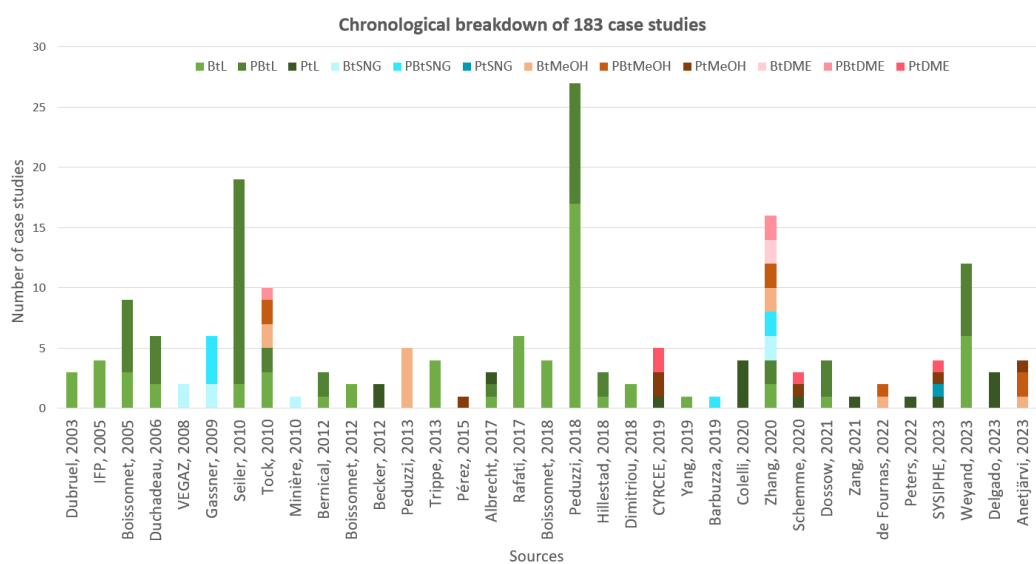


Figure 1: Chronological breakdown of 183 case studies.[22], [10], [11], [23], [jarry•23c•2011], [28], [50], [52], [39], [8], [7], [42], [53], [43], [2], [45], [12], [41], [32], [20], [37], [56], [6], [17], [58], [48], [21], [57], [25], [44], [55], [19]

2 Pathways selection

Thermochemical processes for renewable carbon recovery												
	Inputs	Nb cas	Outputs	Pretreatment	Syngas production	Energy supply	Ratio H/C	Name	Code	Nb of cases (w/o recycling)	Nb of cases (w/ recycling)	ProsimPlus simulation ?
Bt	67	L	Torrefaction	Entrained Flow Gasification	Autothermal	WGS	BIL-TOR-FBG_AUT-WGS	A	9	6	Yes	
				Fluidised Bed Gasification	Autothermal	WGS	BIL-TOR-FBG_AUT-WGS	B	2	1	No	
			Unspecified	Entrained Flow Gasification	Autothermal	WGS	BIL-UNS-FBG_AUT-WGS	C	4	2	No	
			Fluidised Bed Gasification	Autothermal	WGS	BIL-UNS-FBG_AUT-WGS	D	4	6	No		
			Fast Pyrolysis	Entrained Flow Gasification	Autothermal	WGS	BIL-FPY-FBG_AUT-WGS	E	5	3	No	
			Grinding Only	Entrained Flow Gasification	Autothermal	WGS	BIL-GRD-FBG_AUT-WGS	F	2	0	No	
	7	SNG	Fluidised Bed Gasification	Autothermal	WGS	BIL-GRD-FBG_AUT-WGS	G	3	7	No		
			Grinding Only	Fluidised Bed Gasification	Autothermal	TAR	BIL-GRD-FBG_AUT-TAR	H	2	7	No	
			Slow Pyrolysis	Fluidised Bed Gasification	Autothermal	WGS	BISNG-SPY-FBG_AUT-WGS	I	2	0	No	
			Grinding Only	Fluidised Bed Gasification	Autothermal	WGS	BISNG-GRD-FBG_AUT-WGS	J	3	0	Yes	
PBt	15	MeOH	Torrefaction	Entrained Flow Gasification	Autothermal	WGS	BIMeOH-TOR-FBG_AUT-WGS	K	3	0	Yes	
				Fluidised Bed Gasification	Autothermal	WGS	BIMeOH-TOR-FBG_AUT-WGS	L	0	2	No	
			Entrained Flow Gasification	Autothermal	WGS	BIMeOH-SPY-FBG_AUT-WGS	M	1	0	No		
			Grinding Only	Fluidised Bed Gasification	Autothermal	WGS	BIMeOH-GRD-FBG_AUT-WGS	N	2	0	No	
			Non considérée	Flux entrainé	Autothermique	WGS	IDME-UNS-FBG_AUT-WGS-NC	N02	0	0	No	
	53	L	Torrefaction	Entrained Flow Gasification	Autothermal	H2	PBL-TOR-FBG_AUT-H2	O	6	9	Yes	
				Fluidised Bed Gasification	Autothermal	WGS	PBL-TOR-FBG_ALL-WGS	P	1	0	No	
			Unspecified	Entrained Flow Gasification	Autothermal	WGS	PBL-TOR-FBG_ALL-WGS	Q	0	4	No	
			Fluidised Bed Gasification	Autothermal	WGS	PBL-UNS-FBG_ALL-WGS	R	1	0	No		
			Fast Pyrolysis	Entrained Flow Gasification	Autothermal	H2	PBL-FPY-FBG_ALL-H2	S	4	1	No	
Pt	7	SNG	Fluidised Bed Gasification	Autothermal	WGS	PBL-FPY-FBG_ALL-H2	T	2	3	No		
			Grinding Only	Fluidised Bed Gasification	Autothermal	H2	PBL-GRD-FBG_AUT-H2	U	2	5	No	
			Torrefaction	Fluidised Bed Gasification	Autothermal	WGS	PBLSNG-TOR-FBG_ALL-WGS	V	0	5	No	
			Slow Pyrolysis	Fluidised Bed Gasification	Autothermal	WGS	PBLSNG-SPY-FBG_ALL-WGS	W	4	6	No	
			Torrefaction	Fluidised Bed Gasification	Autothermal	WGS	PBLSNG-GRD-FBG_ALL-WGS	X	1	0	No	
	12	MeOH	Torrefaction	Fluidised Bed Gasification	Autothermal	WGS	PBIMeOH-TOR-FBG_ALL-WGS	Y	3	0	No	
			Postcombustion	Co-electrolysis	H2	PIL-PCC-COEL-H2	ZB	3	1	No		
			Postcombustion	Electrolysis	RWGS	PIL-PCC-EL-RWGS	ZC	5	2	Yes		
			Postcombustion	Electrolysis	RWGS	PISNG-PCC-EL-RWGS	ZD	1	0	Yes		
			Postcombustion	Co-electrolysis	H2	PIMeOH-PCC-COEL-H2	ZE	0	1	No		
4	DME	Postcombustion	Co-electrolysis	Electrolysis	H2	PIMeOH-PCC-EL-H2	ZF	0	1	No		
				Electrolysis	RWGS	PIMeOH-PCC-EL-RWGS	ZG	2	0	Yes		
			Electrolysis	Co-electrolysis	H2	PIDME-PCC-COEL-H2	ZH	0	1	No		
				Electrolysis	RWGS	PIDME-PCC-EL-RWGS	ZI	0	1	No		Yes

Figure 2: Specifications of the 37 identified thermochemical conversion processes.

3 Modelling assumptions

Biomass modelling

Biomass is not an existing component in process simulation databases. It has thus been modeled using three existing components, introduced in selected proportions to obtain a mixture with an average atomic composition close to that of lignocellulosic biomass $C_6H_9O_4$. By measuring the LHV of the mix (18.08 MJ.kg $^{-1}$), we define standard enthalpies of formation of the 3 pseudo-components.

Resource processing

Torrefaction is a pre-treatment phase preceding the transportation and gasification of lignocellulosic biomass. It allows for an increase in the H₂ and CO content of syngas by decreasing the O/C ratio of the initial resource [18] and improves biomass grindability [54]. The modeling assumptions for torrefaction are based on two previous internal studies. It involves a simple reactor at 250°C for the torrefaction reaction and a simple reactor at 850°C for the combustion of the fumes produced by the torrefaction. Grinding is a size reduction step required for entrained-flow gasifier technologies (see 3). This

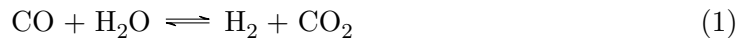
stage is not modeled in the simulations but is included in the economic analysis. E-fuel processes include a post-combustion carbon capture step. It contains a CO₂ absorption phase using an amine solvent at 60°C and a desorption phase to separate the CO₂ and recycle the amine solvent at 110°C. Carbon capture energy requirements are concentrated in the desorption column reboiler [38]. This carbon capture model is inspired by an open-source process example developed by Prosim [15].

Syngas production

Two main biomass gasification technologies coexist in the literature. Fluidized bed gasifiers operate between 800°C and 900°C with a physical separation of the gasification and combustion reactions. In particular, the fluidized bed allows the solid residue formed during gasification to flow into the combustion zone. The separation of the two chambers also enables the separation of the two gas streams produced: syngas and flue gas. This type of technology co-produces a large quantity of methane and is therefore favored for SNG production [39]. Entrained-flow reactors are better suited for high-power industrial plants (> 50MW_{th}). Biomass is injected along with gaseous reactants in a circulating furnace, resulting in partial combustion of the resource. Usually operating at high temperatures (1200 - 1400 °C) to facilitate tar reduction, the entrained-flow reactor is modeled by a balanced reactor minimizing Gibbs free energy, at 1400 °C. Hydrogen production is used in e-fuel and e-biofuel processes as energy carriers for fuel production. A solid oxide electrolysis cells (SOEC) module developed in a previous study [37] is chosen to carry out the simulation. Operating at a high temperature (800°C) means that part of the electrical input required can be replaced by a thermal input, improving the process's energy integration potential [8]. Simulations of biofuel and e-biofuel processes do not require any external heat input, as they produce excess heat power at both low and high temperatures. On the other hand, e-fuel processes require a high-temperature heat input for electrolysis. In the case of the PtL process, this input is provided by the combustion of tail gas at the outlet of the Fischer-Tropsch reactor. For the PtSNG and PtMeOH processes, the heat input is provided by the combustion of the respective products, mainly methane and methanol.

H/C ratio adjustment

The H/C ratio is defined as the H₂ mole fraction over the CO mole fraction. Fuel synthesis requires a specific H/C ratio for optimal performance, between 1.6 and 2.1 depending on the synthesis. For biofuel processes BtL, BtMeOH, BtSNG, H₂ proportion in the syngas needs to be increased. The desired ratio is readjusted with the water-gas-shift (WGS) reaction:



With steam addition and CO molecules, this exothermic reaction ($\Delta H_r^0 = -42 \text{ kJ.mol}^{-1}$) produces extra H₂ and CO₂, resulting in a H/C ratio increasing along with CO₂ losses in the process. The WGS reactor is modeled by a simple reactor operating at 385°C. In the

PtL process, the desired ratio is achieved by shifting the WGS reaction to transform CO₂ into CO, consuming part of the hydrogen supply. This "reverse water-gas shift" reaction requires high pressure and temperature conditions: 25 bar, 600°C [46]. For hybrid processes PBtL, PBtSNG, and PBtMeOH, the quantity of H₂ produced by electrolysis is adjusted to reach the optimal syngas ratio for the fuel synthesis, avoiding CO₂ losses from the WGS reaction.

Fuel synthesis

The liquid hydrocarbon production uses a Fischer-Tropsch reactor, which first converts syngas into C₁ to C₃₀ hydrocarbons. It operates at 220°C in the presence of a cobalt or iron catalyst. The Anderson-Schulz-Flory (ASF) distribution is chosen to describe hydrocarbon production in the Fischer-Tropsch reactor during the polymerization process [36]. The chain growth probability α is set to 0.9 to maximize the production of C₅-C₂₀ carbon chains (naphtha, kerosene, gasoline, diesel). A light gas recycling loop and heavy waxes hydrocracking reactor are modeled to convert C₁-C₄ and C₂₀₊ hydrocarbon chains, increasing production yields [57]. SNG production is carried out with a methanation unit including an olefine reformer and a methanation reactor, both modeled by a constant temperature reactor at 385°C. The methane synthesis is exothermic, which allows heat to be recovered in turbines and provides electrical power for auxiliaries consumption. It involves two main reactions converting CO₂ (Sabatier reaction) or CO (methanation). The methanation unit simulation was previously developed for two internal studies. Finally, methanol synthesis is simulated with a methanolization unit, with a reactor minimizing Gibbs free energy and liquid-vapor separators. The model derives from an open-source process example developed by Prosim and an internal project [37].

Software, thermodynamic model and reactions

Simulations are carried out using a commercial process simulation software – ProSim-Plus® – to allow physical modeling as well as mass and energy balances; modeling is based on standard elementary and user modules and supported by various CEA (French Atomic Energy and Alternative Energies Commission) previous works. The main operating conditions and reactions in each modeled unit are available in Table 1.

4 Performance criteria

Carbon conversion

Biomass and CO₂ from concentrated sources can be considered as carbon resources with limited potential [12]. These limits initially raise the question of how best to allocate these resources prioritizing uses. This issue is especially true for biomass resources, with potential conflicts with the agriculture and forestry sectors [49]. Secondly, it is crucial to

Table 1: Main reactions and operating conditions

Step	Reaction(s)	$P(\text{bar}), T(\text{°C})$
Torrefaction	See section 5.1	1.03, 280
Comb. Biomass 1	$\text{C}_6\text{H}_{10}\text{O}_4 + 6.5 \text{ O}_2 \rightarrow 6 \text{ CO}_2 + 5 \text{ H}_2\text{O}$	1.05, 850
Comb. Biomass 2	$\text{C}_6\text{H}_6\text{O}_3 + 6 \text{ O}_2 \rightarrow 6 \text{ CO}_2 + 3 \text{ H}_2\text{O}$	1.05, 850
Comb. Biomass 3	$\text{C}_6\text{H}_{12}\text{O}_6 + 6 \text{ O}_2 \rightarrow 6 \text{ CO}_2 + 6 \text{ H}_2\text{O}$	1.05, 850
Comb. Methane	$\text{CH}_4 + 2 \text{ O}_2 \rightarrow \text{CO}_2 + 2 \text{ H}_2\text{O}$	1.05, 850
Comb. Acetic acid	$\text{CH}_3\text{COOH} + 2 \text{ O}_2 \rightarrow 2 \text{ CO}_2 + 2 \text{ H}_2\text{O}$	1.05, 850
Gasification EFG	Gibbs free energy minimization	35, 1400
Gasification FICB	See section 5.2	1.5, 800
Water-gas shift	$\text{CO} + \text{H}_2\text{O} \rightarrow \text{CO}_2 + \text{H}_2$	35, 250
Reverse water-gas shift	$\text{CO}_2 + \text{H}_2 \rightarrow \text{CO} + \text{H}_2\text{O}$	25, 600
Fischer-Tropsch	$n\text{CO} + (2n+1) \text{ H}_2 \rightarrow n \text{ H}_2\text{O} + \text{C}_n\text{H}_{2n+2}$ (ASF)	35, 220
Hydrocracking	See section 5.3	50, 50
Methanolization	Gibbs free energy minimization	110, 150
Methanation CO	$\text{CO} + 3 \text{ H}_2 \rightarrow \text{CH}_4 + \text{H}_2\text{O}$	1, 385
Sabatier reaction	$\text{CO}_2 + 4 \text{ H}_2 \rightarrow \text{CH}_4 + 2 \text{ H}_2\text{O}$	1, 385

value limited carbon in the most efficient way possible. This efficiency based on molar flow rates is known as the carbon conversion ratio and is defined as follows:

$$\eta_C = \frac{\dot{m}_{fuels} \cdot M(feedstocks) \cdot \bar{N}_{C-fuels}}{\dot{m}_{feedstocks} \cdot M(fuels) \cdot \bar{N}_{C-feedstocks}} \quad (2)$$

where \dot{m}_{fuels} denotes the mass flow rate of the output products (liquid hydrocarbons, synthetic natural gas, methanol) in $\text{kg} \cdot \text{s}^{-1}$, $\dot{m}_{feedstocks}$ is the mass flow rate of the carbon feedstock, alternatively biomass or carbon dioxide, $M(fuels)$ and $M(feedstocks)$ are the molar mass of the different fuels and feedstocks in $\text{g} \cdot \text{mol}^{-1}$, $\bar{N}_{C-fuels}$ and $\bar{N}_{C-feedstocks}$ are the average number of carbon atoms per molecule of fuel or feedstock. Other indicators are frequently used in the literature, such as material efficiency or chemical energy efficiency [50][41][52][17][20]. They derive directly from the first definition.

Energy efficiency

Energy yield is the performance indicator used to quantify the energy recovery of the resource in the product. It may or may not include auxiliary energy consumption required for process operation. Three definitions coexist in the literature. The internal energy yield η_{int} is expressed as follows:

$$\eta_{int} = \frac{\dot{m}_{fuels} \cdot LHV_{fuels}}{\dot{m}_{biomass} \cdot LHV_{biomass} + P_{electrolysis}} \quad (3)$$

where \dot{m}_{fuels} denotes the mass flow rate of the output products (liquid hydrocarbons, synthetic natural gas, methanol) in $\text{kg} \cdot \text{s}^{-1}$, LHV_{fuels} is the Lower Heating Value (LHV)

of the output products in $\text{MJ} \cdot \text{kg}^{-1}$, $\dot{m}_{biomass}$ is the dry biomass input mass flow rate in $\text{kg} \cdot \text{s}^{-1}$, $LHV_{biomass}$ is the LHV of the dry biomass, and $P_{electrolysis}$ is the electrical power to be supplied for hydrogen production by electrolysis in MW. In biofuel processes $P_{electrolysis} = 0$ whereas in e-fuel processes $\dot{m}_{biomass} = 0$. The overall energy yield $\eta_{ov.}$ is defined by the following formula:

$$\eta_{ov.} = \frac{\dot{m}_{fuels} \cdot LHV_{fuels} + P_{prod-elec}}{\dot{m}_{biomass} \cdot LHV_{biomass} + P_{electrolysis} + P_{aux-elec} + P_{aux-therm}} \quad (4)$$

This efficiency integrates the electrical power recovered from waste heat by turbines $P_{prod-elec}$ and consumed by auxiliary units (compressors, pumps, reboiler) $P_{aux-elec}, P_{aux-therm}$. As most frequently encountered in the literature, we used this efficiency indicator to assess technical performance in this study. After energy integration, potential surplus waste heat is not considered in the calculation of energy yield.

Among the 184 cases reviewed, 174 apply this definition, while 96 use a “primary energy efficiency” that applies a correction factor to electricity (typically 2.6–3). Although such factors reflect the conversion losses of thermal power generation, their applicability depends on system boundaries and electricity generation mixes, and may introduce a bias against electrified pathways. In our context, the indicator is process-based and focuses on the energy content of the produced fuels, which is particularly relevant for hard-to-electrify sectors such as aviation. This metric should therefore be interpreted as one criterion among others in a multi-criteria framework (energy, carbon, economics, environment), and not as a unique measure of energy usefulness. Exergy-based approaches could provide complementary insights, but fall beyond the scope of the present analysis.

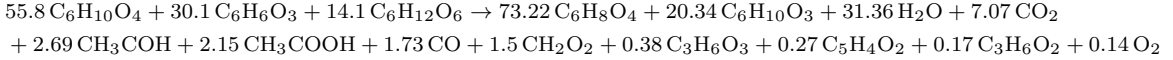
However, to ensure comparability of processes on a primary energy basis, we included a calculation of energy efficiencies assuming four different origins of electricity production: the average European electricity mix, nuclear power, a renewable mix (33% photovoltaic, 33% wind, and 33% hydropower), and combined heat and power (CHP). Accordingly, the electricity consumption of each process was converted using a distinct primary energy factor (PEF) depending on the source of electricity. The selected PEF values and corresponding references are presented in Table 2.

Table 2: Primary energy factors (PEF) used for different electricity sources.

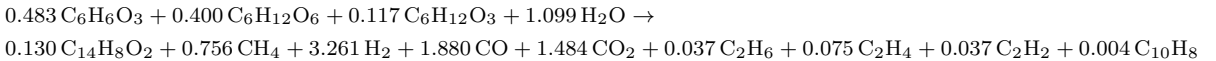
Electricity source	PEF	Ref.
Average EU electricity mix	2.0	[5]
Nuclear power	3.0	[26]
Renewable mix (PV + wind + hydropower)	1.0	[9]
Combined heat and power (CHP)	1.25	[1]

5 Reactions

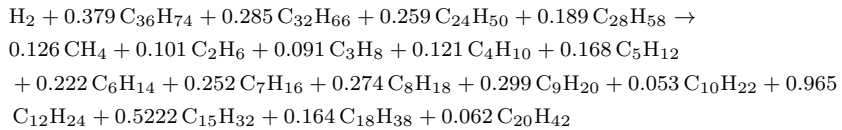
5.1 Torrefaction



5.2 FICB Gasification



5.3 Hydrocracking



6 Economic analysis

6.1 Indicators

Investment costs

Second-generation-type biofuel processes, e-biofuel, and e-fuel processes require heavy transformation infrastructures. The capital intensity C_{int} has a significant impact on the expected production cost. This crucial indicator for potential investors is expressed as follows:

$$C_{int} = \frac{C_{dep}}{\text{Capacity}} \quad (5)$$

with C_{dep} the depreciable capital cost including the cost of equipment, installation, and working capital in €₂₀₂₃ (section 6.2). Installed capacity corresponds to the product output power on LHV basis in kW.

Net production costs

The Net Production Cost (NPC) is useful to compare the estimated competitiveness of the different sectors, relative to market prices. It is calculated as follows:

$$NPC = \frac{C^{fixed} + C^{variable}}{\text{Production}_n} \quad (6)$$

Fixed costs (C^{fixed}) include the depreciation of invested capital, while variable costs ($C^{variable}$) include the cost of inputs (biomass, electricity). The annual production volume of year n $Production_n$ is calculated from material balances of process simulations. The calculation of annualized operating costs is further detailed in section 6.2.

6.2 Economic modeling

The calculation of economic indicators is conducted following the typical economic methodology available in figure 7) [16].

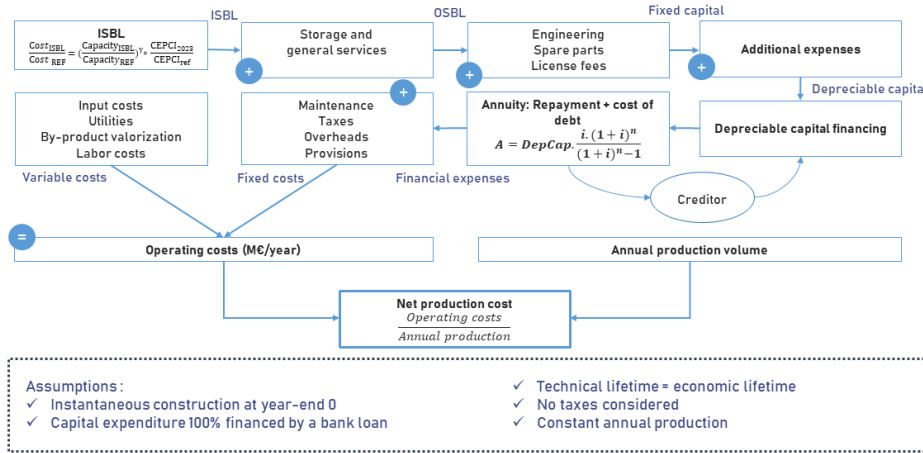


Figure 3: Net production cost calculation methodology

Equipment costs

The cost of industrial equipment is estimated with a reference cost and a scale factor γ allowing extrapolation relative to the capacity of the installed equipment. Costs were updated using values from the Chemical Engineering Plant Cost Index (CEPCI). In the study, we gathered several reference costs for the same industrial equipment. Values provided by different studies can often differ significantly, depending on the chosen assumptions. An arbitration was conducted to select a reference value for each technological component of our processes. The scale factor is specific to each equipment and is usually specified in the source study. In the absence of details, we applied a standard value of 0.7 for the scale factor. The list of equipment required in the simulated processes and their associated reference costs are specified in Table 3.

The "Inside Battery Limit" (ISBL) cost of each piece of equipment is defined as

follows :

$$\frac{\text{Cost}_{\text{ISBL}}}{\text{Cost}_{\text{Ref.}}} = \left(\frac{\text{Capacity}_{\text{ISBL}}}{\text{Capacity}_{\text{Ref.}}} \right)^\gamma \times \frac{\text{CEPCI}_{2023}}{\text{CEPCI}_{\text{Ref.}}} \quad (7)$$

Due to a lack of data, extrapolations in this study may exceed the recommended duration of 5 years for cost updating. This recommendation does not seem to be particularly respected in the literature.

Investment costs

In addition to ISBL costs, the fixed capital cost includes the cost of utilities and control, piping, storage, buildings and infrastructure, engineering, risk provisions, and licenses. According to [29] the factor between the ISBL cost and fixed capital is typically ranging from 1.8 to 2.5 in the associated literature. The estimation of each expense item is typically expressed as a percentage of the ISBL cost. By cross-comparison of assumptions made by studies in the literature with those chosen in [16], typical values are selected for this study and presented in Table 8.

Under these assumptions, the installation factor between the ISBL equipment cost and the fixed capital reaches 2.25. The depreciable capital is obtained by adding startup costs and loan interests.

Industrial-scale Fischer-Tropsch units generally have input capacities between 200 and 500 MW, corresponding to dry biomass inputs between 40 and 100 t/h for biofuel processes [24]. On average, SNG synthesis units are smaller with input capacities between 20 and 100 MW [35]. Finally, for methanol synthesis, we find rather low values of around 20 MW for BtMeOH and PBtMeOH processes [42] and rather high values of around 500 MW for PtMeOH processes [43]. These values correspond to capacities for industrial units and are not based on real operational units, as the industrial deployment of this type of technology is still in its infancy [14]. The sizing of each installation is detailed in the Table 6.

Fixed costs

As most frequently encountered in the literature, a net production cost (NPC) calculation is chosen over the Levelized Cost of Production (LCOP) method [30]. Constant annual operating costs approximation is valid under specific assumptions :

- The construction of the facilities is instantaneous, at the end of year 0.
- Depreciable capital is 100% financed by debt, with a chosen fixed interest rate.
- The loan repayment period is equal to the depreciation period of the capital and the technical lifespan of the facilities.
- No taxes are applied.

- Annual fuel production is assumed to be constant over the entire lifespan of the facilities.

Under these assumptions the debt is repaid with interest in the form of annuities, calculated as follows:

$$A = C_{dep} \cdot \frac{i \cdot (1 + i)^n}{(1 + i)^n - 1} \quad (8)$$

A is the annuity representing the financial burden, C_{dep} is the value of the depreciable capital of the project in million euros (M€), i is the bank loan interest rate, and n is the lifespan and repayment period of the installation in years. Other fixed costs are taken into account: maintenance, property taxes, insurance, and overhead. The values chosen for these expenses are based on those most commonly found in the literature and are specified in Table 4. They are expressed as a fraction of the ISBL (+ Utilities) cost or fixed capital. Finally, the cost of labor is estimated by considering a need for k operators (where k varies depending on the size of the unit), remunerated at 60 k€ per year, and present on-site for 8 hours per day in shifts. To take into account rest times, we applied 4.56 multiplication factor [27].

Variable costs

In the context of our study, the primary inputs include dry biomass, electricity, natural gas, and water. Paraffin wax is also used in the BtSNG and PBtSNG processes during the fluidized bed reactor gasification stage. The cost of catalysts is disregarded. Dry biomass is traded in the form of woodchips. The woodchip purchase price reflects the costs of cutting, drying, grinding, and transporting the resource. It is set in the study as a frequently encountered literature value [2][41][3]. The prices of electricity and natural gas are average market prices (EPEX spot for electricity, PEG for natural gas) for the year 2023. The paraffin wax price is taken from the Paraffin price index, in Europe.

7 Reference costs and dimensions of equipment

Table 3: Reference costs and dimensions of the main transformation units.

Unit	Cost (M€)	Size	Unit	γ	Year	CEPCI	Source
Torrefaction	13,21	100	kt.year^{-1}	0,7	2011	585,7	[25]
Grinding	0,75	200	MW_{th} LHV	0,6	2002	395,6	[45]
Drying	16,69	200	MW_{th} LHV	0,8	2002	395,6	[45]
Carbon capture	58,01	2709	$\text{kmol CO}_2.\text{h}^{-1}$	0,7	2012	708,8	[4]
EF reactor	54,59	432	MW_{th}	0,7	2012	584,6	[40]
FICB reactor	35,43	68,8	t.h^{-1}	0,7	2001	394,3	[31]
Quench	0,33	3,743	$\text{m}^3.\text{s}^{-1}$	0,67	2012	584,6	[40]
ASU	29,11	576	t.day^{-1}	0,75	2012	584,6	[40]
WGS	13,39	8819	kmol.h^{-1}	0,65	2002	395,6	[25]
RWGS	37,47	4000	kmol.h^{-1}	0,7	2019	607,5	[57]
SOEC	0,48	1	MW_{el}	1	2019	607,5	[34]
AGR	4,54	542	$\text{kmol CO}_2.\text{h}^{-1}$	0,75	2012	584,6	[40]
FT reactor	11,21	0,9025	kmol.s^{-1}	0,67	2014	576,1	[40]
SNG synthesis	5,23	175	MW_{out} HHV	0,75	2012	584,6	[33]
MeOH synthesis	76,05	10,81	kmol.s^{-1}	0,7	2002	395,6	[33]
Hydrocracking	12,00	19,7	t.h^{-1}	0,7	2010	550,8	[51]
Compressor	6,31	10	MW_{el}	0,67	2007	525,4	[25]
Exchanger	18,10	355	MW_{th}	0,7	2007	525,4	[25]
MeOH purification	1,60	4,66	kg.s^{-1}	0,291	2002	395,6	[33]

8 Additional costs

Expense	Cost
Utilities and control	0.2 ISBL
Piping	0.15 ISBL
Storage	0.25 ISBL
Building and infrastructure	0.2 ISBL
Engineering	0.2 ISBL
Contingencies	0.25 ISBL

Table 4: Expense breakdown and corresponding costs.

9 GHG analysis assumptions

Feedstock	Emission factor (kgCO _{2,eq} /MWh)	Reference
Biomass (< 500 km)	26.4	RED III
Electricity (2022, France)	54.4	RTE
Electricity (2050, France)	13.0	RTE [47]
Electricity (2023, EU average)	326	RTE
Electricity (nuclear)	6.0	UNECE, 2022
Electricity (33% PV, 33% wind, 33% hydro)	18	UNECE, 2022
Electricity (CHP)	322	[13]
Natural gas	197.8	Chiffres clés du climat, 2023
Waxes	327.6	ADEME, Base Carbone

Table 5: Reference and alternative emission factors for the different contributing feedstocks.

10 Simulation input sizing

Table 6: Biomass and power inputs of the 9 processes.

Process	Biomass input (MW _{th})	Electrolysis input (MW _{el})
BtL	436	0
PBtL	436	268
PtL	0	566
BtSNG	67	0
PBtSNG	67	57,8
PtSNG	0	57,8
BtMeOH	436	0
PBtMeOH	436	244
PtMeOH	0	501

11 Sensitivity on energy efficiency

Table 7: Primary energy efficiency of each process under different electricity supply assumptions and their primary energy factor (PEF).

Process	Primary energy efficiency			
	EU mix (PEF 2.0)	Nuclear (PEF 3.0)	Renewable mix (PEF 1.0)	CHP (PEF 1.25)
BtL	47.1%	45.9%	48.3%	48.0%
PBtL	41.5%	32.6%	57.3%	52.4%
PtL	26.1%	17.9%	48.5%	39.9%
BtSNG	46.5%	45.7%	47.4%	47.2%
PBtSNG	45.9%	36.3%	64.0%	58.1%
PtSNG	35.6%	25.5%	61.2%	51.6%
BtMeOH	52.5%	50.5%	54.7%	54.2%
PBtMeOH	45.9%	35.9%	63.5%	58.0%
PtMeOH	31.8%	22.4%	54.7%	46.4%

Note: PEF stands for Primary Energy Factor, which converts final electricity into its primary energy equivalent.

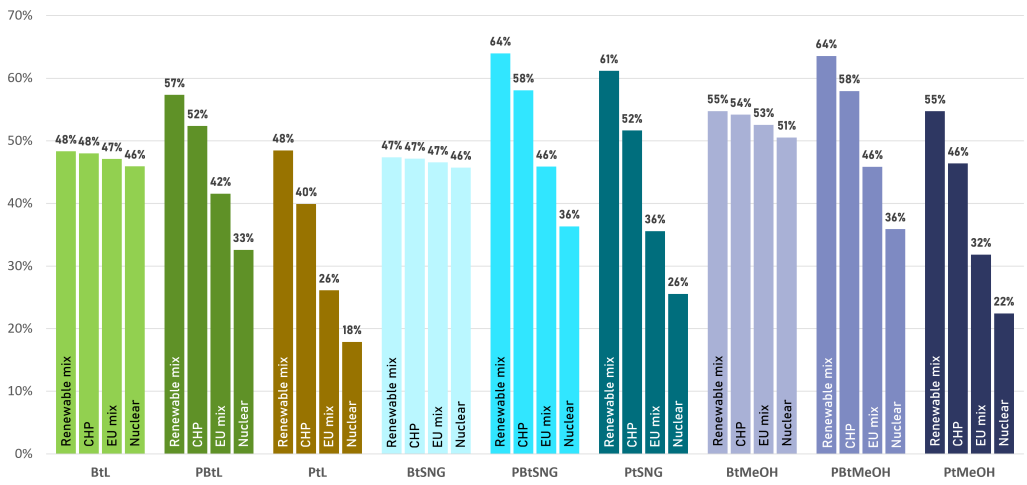


Figure 4: Evolution of the primary energy efficiency of each process under different electricity supply assumptions.

12 Production costs sensitivity

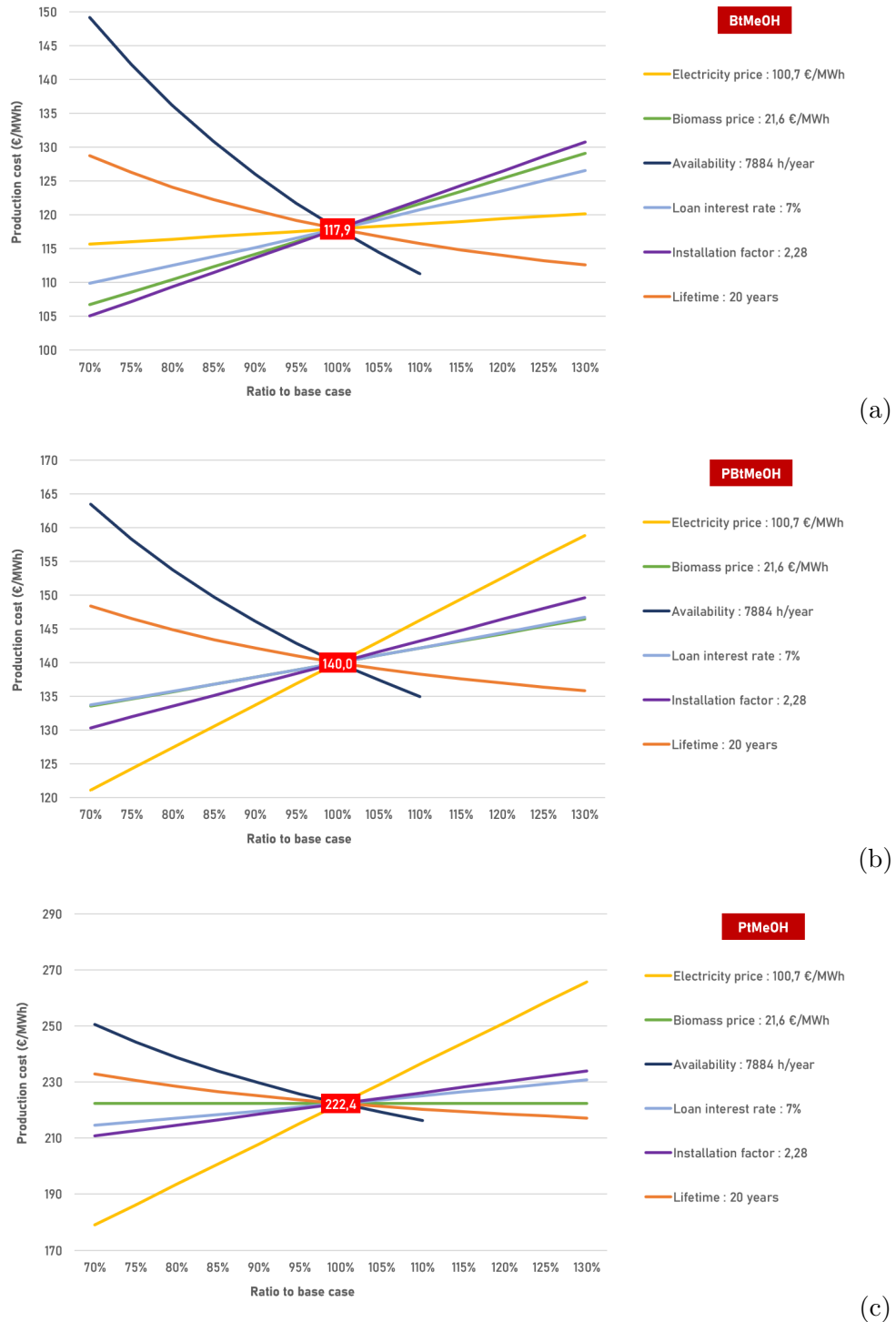
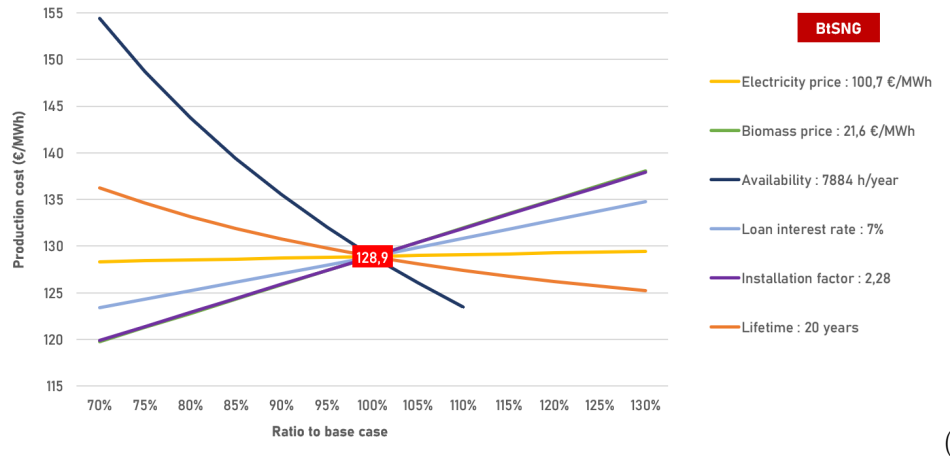
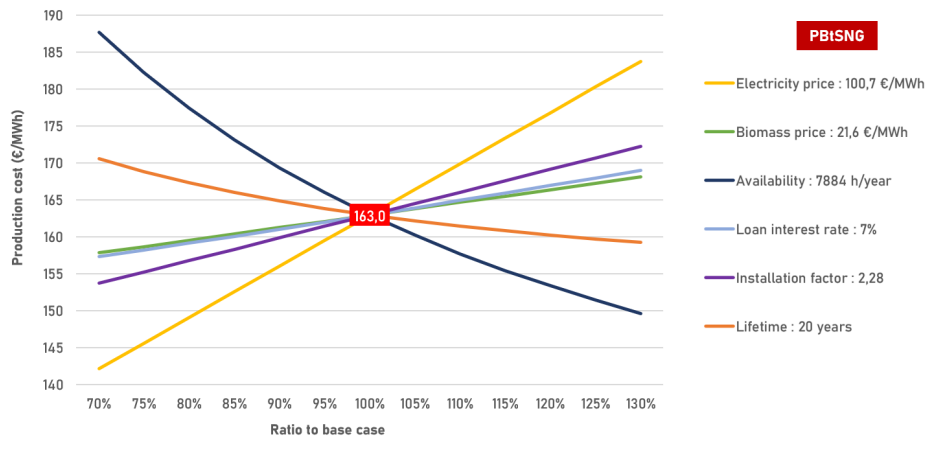


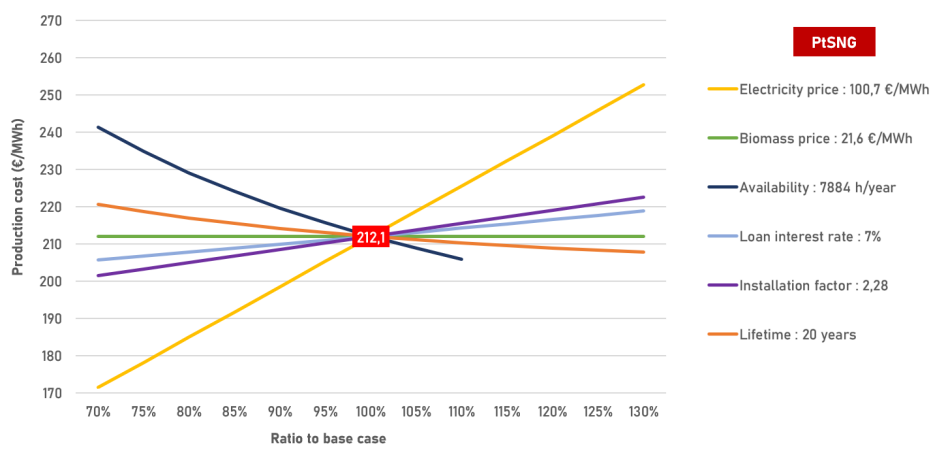
Figure 5: Sensitivity analysis on net production cost for BtMeOH (a), PBtMeOH (b), and PtMeOH (c) processes



(d)



(e)



(f)

Figure 6: Sensitivity analysis on net production cost for BtSNG (d), PBtSNG (e) and PtSNG (f) processes

13 GHG sensitivity analysis

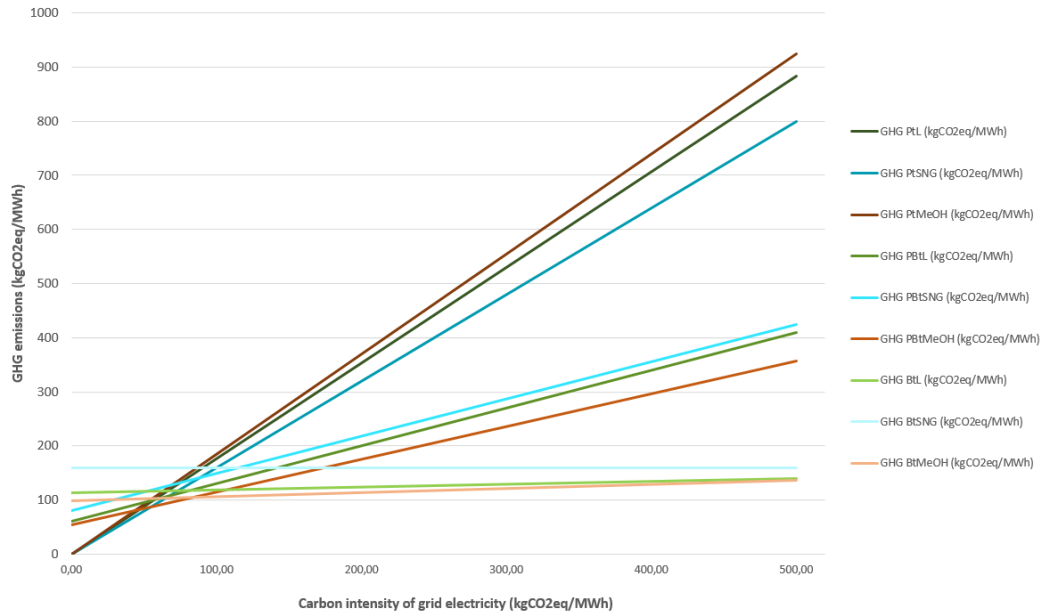


Figure 7: BtX, PBtX and PtX GHG emission sensitivity with respect to electricity carbon intensity

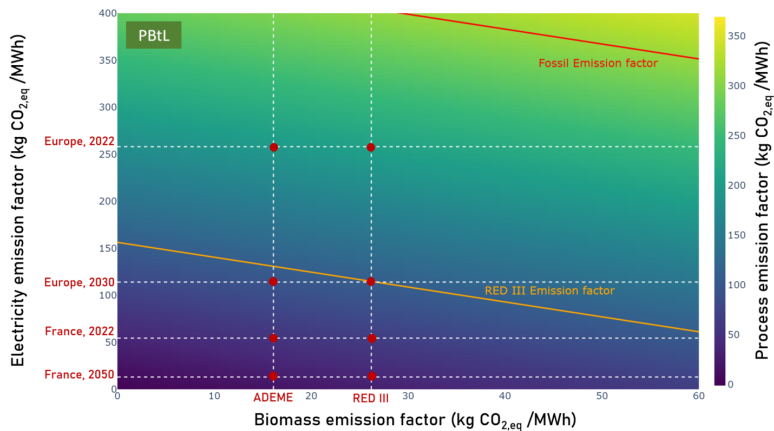


Figure 8: Cross-sensitivity analysis of PBtL GHG emissions depending on electricity and biomass emission factor. The red line represents the emission level of a fossil equivalent. The orange line represents the maximum permissible level of emissions to meet RED III requirements.

Table 8: GHG emissions of each process (kgCO₂eq/MWh) under different electricity mixes and biomass emission factor sources (ADEME and RED III). Values are coloured according to compliance with RED II sustainability thresholds.

Process	GHG emissions of process (kgCO ₂ eq/MWh)							
	Biomass EF source: ADEME				Biomass EF source: RED III			
	EU mix	Nuclear	Renew. mix	CHP	EU mix	Nuclear	Renew. mix	CHP
BtL	50.90	33.52	34.20	50.70	72.11	54.73	55.41	71.91
PBtL	245.54	21.67	30.41	242.95	256.92	33.05	41.79	254.33
PtL	575.04	9.71	31.78	568.50	575.04	9.71	31.78	568.50
BtSNG	95.29	95.29	95.29	95.29	112.29	112.29	112.29	112.29
PBtSNG	272.76	52.28	60.89	270.20	281.41	60.93	69.54	278.86
PtSNG	520.62	8.79	28.77	514.70	520.62	8.79	28.77	514.70
BtMeOH	53.65	29.29	30.24	53.37	72.08	47.72	47.72	71.80
PBtMeOH	213.60	19.29	26.87	211.35	223.78	29.47	29.47	221.53
PtMeOH	602.03	10.17	33.27	595.18	602.03	10.17	10.17	595.18

Note: Values represent process GHG emissions expressed per unit of final energy output (kgCO₂eq/MWh), calculated for different electricity mixes and biomass emission factor (EF) sources. **Green** values are **below the RED II sustainability threshold**, while **red** values **exceed it**. Thresholds correspond to at least **65% GHG reduction** for biofuels and e-biofuels, and **70% reduction** for e-fuels compared to fossil equivalents.

Thresholds applied: 109.24 (BtL, PBtL), 93.64 (PtL), 86.40 (BtSNG, PBtSNG, PtSNG), 86.94 (BtMeOH, PBtMeOH), and 74.52 kgCO₂eq/MWh (PtMeOH).

References

- [1] AEBIOM. *PRIMARY ENERGY FACTOR FOR ELECTRICITY IN THE ENERGY EFFICIENCY DIRECTIVE*. Tech. rep. 2017.
- [2] Friedemann G. Albrecht et al. “A standardized methodology for the techno-economic evaluation of alternative fuels – A case study”. en. In: *Fuel* 194 (Apr. 2017), pp. 511–526. ISSN: 00162361. DOI: 10.1016/j.fuel.2016.12.003. URL: <https://linkinghub.elsevier.com/retrieve/pii/S0016236116312248> (visited on 07/07/2023).
- [3] Eemeli Anetjärvi, Esa Vakkilainen, and Kristian Melin. “Benefits of hybrid production of e-methanol in connection with biomass gasification”. en. In: *Energy* 276 (Aug. 2023), p. 127202. ISSN: 03605442. DOI: 10.1016/j.energy.2023.127202. URL: <https://linkinghub.elsevier.com/retrieve/pii/S0360544223005960> (visited on 08/24/2023).
- [4] Solomon Aforkoghene Aromada, Nils Henrik Eldrup, and Lars Erik Øi. “Capital cost estimation of CO₂ capture plant using Enhanced Detailed Factor (EDF) method: Installation factors and plant construction characteristic factors”. en. In: *International Journal of Greenhouse Gas Control* 110 (Sept. 2021), p. 103394. ISSN: 17505836. DOI: 10.1016/j.ijggc.2021.103394. URL: <https://linkinghub.elsevier.com/retrieve/pii/S1750583621001468> (visited on 09/18/2023).
- [5] Constantinos A. Balaras et al. “Primary Energy Factors for Electricity Production in Europe”. en. In: *Energies* 16.1 (Dec. 2022), p. 93. ISSN: 1996-1073. DOI: 10.3390/en16010093. URL: <https://www.mdpi.com/1996-1073/16/1/93> (visited on 10/29/2025).
- [6] Eleonora Barbusza et al. “Gasification of wood biomass with renewable hydrogen for the production of synthetic natural gas”. en. In: *Fuel* 242 (Apr. 2019), pp. 520–531. ISSN: 00162361. DOI: 10.1016/j.fuel.2019.01.079. URL: <https://linkinghub.elsevier.com/retrieve/pii/S0016236119300791> (visited on 08/24/2023).
- [7] W.L. Becker et al. “Production of Fischer–Tropsch liquid fuels from high temperature solid oxide co-electrolysis units”. en. In: *Energy* 47.1 (Nov. 2012). Number: 1, pp. 99–115. ISSN: 03605442. DOI: 10.1016/j.energy.2012.08.047. URL: <https://linkinghub.elsevier.com/retrieve/pii/S0360544212006792> (visited on 07/07/2023).
- [8] Quentin Bernical et al. “Sustainability Assessment of an Integrated High Temperature Steam Electrolysis-Enhanced Biomass to Liquid Fuel Process”. en. In: *Industrial & Engineering Chemistry Research* 52.22 (June 2013). Number: 22, pp. 7189–7195. ISSN: 0888-5885, 1520-5045. DOI: 10.1021/ie302490y. URL: [tock](https://doi.org/10.1021/ie302490y) (visited on 07/07/2023).

[9] Matteo Bilardo, Sara Galatà, and Enrico Fabrizio. “The role of Primary Energy Factors (PEF) for electricity in the evaluation and comparison of building energy performance: An investigation on European nZEBs according to EN 17423:2020”. en. In: *Sustainable Cities and Society* 87 (Dec. 2022), p. 104189. ISSN: 22106707. DOI: 10.1016/j.scs.2022.104189. URL: <https://linkinghub.elsevier.com/retrieve/pii/S2210670722005029> (visited on 10/31/2025).

[10] Boissonnet. *Production d'un carburant de synthèse issu de la gazéification de la biomasse : évaluation du procédé par simulation*. 2005.

[11] Guillaume Boissonnet. *Comparaison de plusieurs procédés de gazéification de la biomasse en vue de produire des carburants liquides de type Fischer-Tropsch*. Tech. rep. 2005.

[12] Guillaume Boissonnet. *La biomasse dans le système énergétique français*. Presenters: _:n333. 2019.

[13] Nadja Buchenau et al. “Allocation of carbon dioxide emissions to the by-products of combined heat and power plants: A methodological guidance”. en. In: *Renewable and Sustainable Energy Transition* 4 (Aug. 2023), p. 100069. ISSN: 2667095X. DOI: 10.1016/j.rset.2023.100069. URL: <https://linkinghub.elsevier.com/retrieve/pii/S2667095X23000259> (visited on 10/31/2025).

[14] Vincent Capo-Canellas. *Décarbonation des transports : l'urgence de choisir, développer des filières de carburants et d'hydrogène durables*. Mission d'information. Sénat: Sénat, July 2023.

[15] *CAPTURE DU CO₂ PAR UNE SOLUTION AQUEUSE D'AMINE*. 2021.

[16] A. Chauvel, G. Fournier, and C. Raimbault. *Manuel d'évaluation économique des procédés*. 2001.

[17] Leonardo Colelli et al. “E-fuels, technical and economic analysis of the production of synthetic kerosene precursor as sustainable aviation fuel”. en. In: *Energy Conversion and Management* 288 (July 2023), p. 117165. ISSN: 01968904. DOI: 10.1016/j.enconman.2023.117165. URL: <https://linkinghub.elsevier.com/retrieve/pii/S0196890423005113> (visited on 07/13/2023).

[18] C. Couhert, S. Salvador, and J-M. Commandré. “Impact of torrefaction on syngas production from wood”. en. In: *Fuel* 88.11 (Nov. 2009), pp. 2286–2290. ISSN: 00162361. DOI: 10.1016/j.fuel.2009.05.003. URL: <https://linkinghub.elsevier.com/retrieve/pii/S001623610900235X> (visited on 02/23/2024).

[19] Hernan E. Delgado et al. “Techno-economic analysis and life cycle analysis of e-fuel production using nuclear energy”. en. In: *Journal of CO₂ Utilization* 72 (June 2023), p. 102481. ISSN: 22129820. DOI: 10.1016/j.jcou.2023.102481. URL: <https://linkinghub.elsevier.com/retrieve/pii/S2212982023000926> (visited on 07/07/2023).

[20] Ioanna Dimitriou, Harry Goldingay, and Anthony V. Bridgwater. “Techno-economic and uncertainty analysis of Biomass to Liquid (BTL) systems for transport fuel production”. en. In: *Renewable and Sustainable Energy Reviews* 88 (May 2018), pp. 160–175. ISSN: 13640321. DOI: 10.1016/j.rser.2018.02.023. URL: <https://linkinghub.elsevier.com/retrieve/pii/S1364032118300492> (visited on 07/07/2023).

[21] Marcel Dossow et al. “Improving carbon efficiency for an advanced Biomass-to-Liquid process using hydrogen and oxygen from electrolysis”. en. In: *Renewable and Sustainable Energy Reviews* 152 (Dec. 2021), p. 111670. ISSN: 13640321. DOI: 10.1016/j.rser.2021.111670. URL: <https://linkinghub.elsevier.com/retrieve/pii/S1364032121009424> (visited on 07/07/2023).

[22] Marie Dubruel. *SIMULATION D’UN PROCEDE DE GAZEIFICATION DE LA BIOMASSE ET DE SYNTHESE DE CARBURANTS FISCHER-TROPSCH*. Tech. rep. 2003.

[23] A. Duchadeau. *Comparaison de schémas de procédés de gazéification de la biomasse par simulation*. Tech. rep. 2006.

[24] C.W. Forsberg et al. “Replacing liquid fossil fuels and hydrocarbon chemical feedstocks with liquid biofuels from large-scale nuclear biorefineries”. en. In: *Applied Energy* 298 (Sept. 2021), p. 117225. ISSN: 03062619. DOI: 10.1016/j.apenergy.2021.117225. URL: <https://linkinghub.elsevier.com/retrieve/pii/S0306261921006486> (visited on 07/07/2023).

[25] Nicolas de Fournas and Max Wei. “Techno-economic assessment of renewable methanol from biomass gasification and PEM electrolysis for decarbonization of the maritime sector in California”. en. In: *Energy Conversion and Management* 257 (Apr. 2022), p. 115440. ISSN: 01968904. DOI: 10.1016/j.enconman.2022.115440. URL: <https://linkinghub.elsevier.com/retrieve/pii/S0196890422002369> (visited on 08/24/2023).

[26] Fraunhofer. *Energy explained - Primary Energy Factors*. Tech. rep. 2023.

[27] Martin Gassner. “Process Design Methodology for Thermochemical Production of Fuels from Biomass. Application to the Production of Synthetic Natural Gas from Lignocellulosic Resources”. PhD thesis. 2010.

[28] Martin Gassner and François Maréchal. “Thermo-economic process model for thermochemical production of Synthetic Natural Gas (SNG) from lignocellulosic biomass”. en. In: *Biomass and Bioenergy* 33.11 (Nov. 2009). Number: 11, pp. 1587–1604. ISSN: 09619534. DOI: 10.1016/j.biombioe.2009.08.004. URL: <https://linkinghub.elsevier.com/retrieve/pii/S0961953409001639> (visited on 07/07/2023).

[29] Geert Haarlemmer et al. “Investment and production costs of synthetic fuels – A literature survey”. en. In: *Energy* 66 (Mar. 2014), pp. 667–676. ISSN: 03605442. DOI: 10.1016/j.energy.2014.01.093. URL: <https://linkinghub.elsevier.com/retrieve/pii/S0360544214001157> (visited on 07/07/2023).

[30] Geert Haarlemmer et al. “Second generation BtL type biofuels – a production cost analysis”. en. In: *Energy & Environmental Science* 5.9 (2012). Number: 9, p. 8445. ISSN: 1754-5692, 1754-5706. DOI: 10.1039/c2ee21750c. URL: <http://xlink.rsc.org/?DOI=c2ee21750c> (visited on 07/07/2023).

[31] C Hamelinck et al. “Production of FT transportation fuels from biomass; technical options, process analysis and optimisation, and development potential”. In: *Energy* 29.11 (Sept. 2004), pp. 1743–1771. ISSN: 03605442. DOI: 10.1016/j.energy.2004.01.002. URL: <https://linkinghub.elsevier.com/retrieve/pii/S0360544204000027> (visited on 09/12/2023).

[32] M. Hillestad et al. “Improving carbon efficiency and profitability of the biomass to liquid process with hydrogen from renewable power”. en. In: *Fuel* 234 (Dec. 2018), pp. 1431–1451. ISSN: 00162361. DOI: 10.1016/j.fuel.2018.08.004. URL: <https://linkinghub.elsevier.com/retrieve/pii/S0016236118313632> (visited on 07/07/2023).

[33] Kristina M Holmgren. *Investment cost estimates for gasification-based biofuel production systems*. Tech. rep. Aug. 2015.

[34] Dohyung Jang et al. “Techno-economic analysis and Monte Carlo simulation of green hydrogen production technology through various water electrolysis technologies”. en. In: *Energy Conversion and Management* 258 (Apr. 2022), p. 115499. ISSN: 01968904. DOI: 10.1016/j.enconman.2022.115499. URL: <https://linkinghub.elsevier.com/retrieve/pii/S0196890422002953> (visited on 09/14/2023).

[35] Daria Katla et al. “Preliminary experimental study of a methanation reactor for conversion of H₂ and CO₂ into synthetic natural gas (SNG)”. en. In: *Energy* 263 (Jan. 2023), p. 125881. ISSN: 03605442. DOI: 10.1016/j.energy.2022.125881. URL: <https://linkinghub.elsevier.com/retrieve/pii/S0360544222027670> (visited on 09/07/2023).

[36] Arno De Klerk. “Fischer–Tropsch fuels refinery design”. en. In: *Energy & Environmental Science* 4.4 (2011), p. 1177. ISSN: 1754-5692, 1754-5706. DOI: 10.1039/c0ee00692k. URL: <http://xlink.rsc.org/?DOI=c0ee00692k> (visited on 02/01/2024).

[37] E. Le Goff. *Etude technico-économique de filières de valorisation de CO₂ sous forme de produits chimiques liquides à partir de la technologie SOEC*. Tech. rep. 2019.

[38] Jan Mertens et al. “Carbon capture and utilization: More than hiding CO₂ for some time”. en. In: *Joule* 7.3 (Mar. 2023), pp. 442–449. ISSN: 25424351. DOI: 10.1016/j.joule.2023.01.005. URL: <https://linkinghub.elsevier.com/retrieve/pii/S2542435123000363> (visited on 07/07/2023).

[39] Marie Minière. *Simulation et évaluation technico-économique de la filière de production de SNG à partir de biomasse*. Tech. rep.

[40] Emanuela Peduzzi. “Biomass to Liquids: Thermo-Economic Analysis and Multi-Objective Optimisation”. PhD Thesis. EPFL, 2015.

[41] Emanuela Peduzzi et al. “Thermo-economic analysis and multi-objective optimisation of lignocellulosic biomass conversion to Fischer–Tropsch fuels”. en. In: *Sustainable Energy & Fuels* 2.5 (2018). Number: 5, pp. 1069–1084. ISSN: 2398-4902. DOI: 10.1039/C7SE00468K. URL: <http://xlink.rsc.org/?DOI=C7SE00468K> (visited on 07/07/2023).

[42] Emanuela Peduzzi et al. “Thermo-economic evaluation and optimization of the thermo-chemical conversion of biomass into methanol”. en. In: *Energy* 58 (Sept. 2013), pp. 9–16. ISSN: 03605442. DOI: 10.1016/j.energy.2013.05.029. URL: <https://linkinghub.elsevier.com/retrieve/pii/S0360544213004398> (visited on 07/07/2023).

[43] Mar Pérez-Fortes et al. “Methanol synthesis using captured CO₂ as raw material: Techno-economic and environmental assessment”. In: *Applied Energy* 161 (Jan. 2016), pp. 718–732. ISSN: 03062619. DOI: 10.1016/j.apenergy.2015.07.067. URL: <https://linkinghub.elsevier.com/retrieve/pii/S0306261915009071> (visited on 07/13/2023).

[44] Ralf Peters et al. “A Techno-Economic Assessment of Fischer–Tropsch Fuels Based on Syngas from Co-Electrolysis”. en. In: *Processes* 10.4 (Apr. 2022), p. 699. ISSN: 2227-9717. DOI: 10.3390/pr10040699. URL: <https://www.mdpi.com/2227-9717/10/4/699> (visited on 01/30/2024).

[45] Mohammad Rafati et al. “Techno-economic analysis of production of Fischer–Tropsch liquids via biomass gasification: The effects of Fischer–Tropsch catalysts and natural gas co-feeding”. In: *Energy Conversion and Management* 133 (Feb. 2017), pp. 153–166. ISSN: 01968904. DOI: 10.1016/j.enconman.2016.11.051. URL: <https://linkinghub.elsevier.com/retrieve/pii/S0196890416310603> (visited on 07/07/2023).

[46] Ebrahim Rezaei and Stephen Dzuryk. “Techno-economic comparison of reverse water gas shift reaction to steam and dry methane reforming reactions for syngas production”. en. In: *Chemical Engineering Research and Design* 144 (Apr. 2019), pp. 354–369. ISSN: 02638762. DOI: 10.1016/j.cherd.2019.02.005. URL: <https://linkinghub.elsevier.com/retrieve/pii/S0263876219300516> (visited on 09/18/2023).

[47] RTE, DiESE. *Futurs énergétiques*. Tech. rep. 2021.

[48] Steffen Schemme et al. “H₂-based synthetic fuels: A techno-economic comparison of alcohol, ether and hydrocarbon production”. In: *International Journal of Hydrogen Energy* 45.8 (Feb. 2020), pp. 5395–5414. ISSN: 03603199. DOI: 10.1016/j.ijhydene.2019.05.028. URL: <https://linkinghub.elsevier.com/retrieve/pii/S0360319919318580> (visited on 01/30/2024).

[49] Comité de prospective en énergie de l’Académie des sciences. *Quelles perspectives énergétiques pour la biomasse ?* Tech. rep. Académie des Sciences, 2024.

[50] Jean-Marie Seiler et al. “Technical and economical evaluation of enhanced biomass to liquid fuel processes”. en. In: *Energy* 35.9 (Sept. 2010). Number: 9, pp. 3587–3592. ISSN: 03605442. DOI: 10.1016/j.energy.2010.04.048. URL: <https://linkinghub.elsevier.com/retrieve/pii/S0360544210002562> (visited on 07/07/2023).

[51] M Tijmensen. “Exploration of the possibilities for production of Fischer Tropsch liquids and power via biomass gasification”. In: *Biomass and Bioenergy* 23.2 (Aug. 2002). Number: 2, pp. 129–152. ISSN: 09619534. DOI: 10.1016/S0961-9534(02)00037-5. URL: <https://linkinghub.elsevier.com/retrieve/pii/S0961953402000375> (visited on 09/12/2023).

[52] Laurence Tock, Martin Gassner, and François Maréchal. “Thermochemical production of liquid fuels from biomass: Thermo-economic modeling, process design and process integration analysis”. In: *Biomass and Bioenergy* 34.12 (Dec. 2010), pp. 1838–1854. ISSN: 09619534. DOI: 10.1016/j.biombioe.2010.07.018. URL: <https://linkinghub.elsevier.com/retrieve/pii/S0961953410002424> (visited on 07/07/2023).

[53] Frederik Trippe et al. “Comprehensive techno-economic assessment of dimethyl ether (DME) synthesis and Fischer–Tropsch synthesis as alternative process steps within biomass-to-liquid production”. en. In: *Fuel Processing Technology* 106 (Feb. 2013), pp. 577–586. ISSN: 03783820. DOI: 10.1016/j.fuproc.2012.09.029. URL: <https://linkinghub.elsevier.com/retrieve/pii/S0378382012003451> (visited on 07/07/2023).

[54] L. Wang et al. “Effect of torrefaction on physiochemical characteristics and grindability of stem wood, stump and bark”. en. In: *Applied Energy* 227 (Oct. 2018), pp. 137–148. ISSN: 03062619. DOI: 10.1016/j.apenergy.2017.07.024. URL: <https://linkinghub.elsevier.com/retrieve/pii/S0306261917308930> (visited on 05/23/2024).

[55] Julia Weyand, Felix Habermeyer, and Ralph-Uwe Dietrich. “Process design analysis of a hybrid power-and-biomass-to-liquid process – An approach combining life cycle and techno-economic assessment”. In: *Fuel* 342 (June 2023), p. 127763. ISSN: 00162361. DOI: 10.1016/j.fuel.2023.127763. URL: <https://linkinghub.elsevier.com/retrieve/pii/S0016236123003769> (visited on 07/07/2023).

[56] Shiying Yang, Yucheng Yang, and Yongjun Liu. “The value-added of dual-stage entrained flow gasification and CO₂ cycling in biomass-to-gasoline/diesel: Design and techno-economic analysis”. en. In: *Computers & Chemical Engineering* 128 (Sept. 2019), pp. 106–116. ISSN: 00981354. DOI: 10.1016/j.compchemeng.2019.05.031. URL: <https://linkinghub.elsevier.com/retrieve/pii/S0098135418311372> (visited on 07/07/2023).

[57] Guiyan Zang et al. “Performance and cost analysis of liquid fuel production from H₂ and CO₂ based on the Fischer-Tropsch process”. en. In: *Journal of CO₂ Utilization* 46 (Apr. 2021), p. 101459. ISSN: 22129820. DOI: 10.1016/j.jcou.

2021 . 101459. URL: <https://linkinghub.elsevier.com/retrieve/pii/S2212982021000263> (visited on 07/07/2023).

[58] Hanfei Zhang et al. “Techno-economic evaluation of biomass-to-fuels with solid-oxide electrolyzer”. en. In: *Applied Energy* 270 (July 2020), p. 115113. ISSN: 03062619. DOI: 10.1016/j.apenergy.2020.115113. URL: <https://linkinghub.elsevier.com/retrieve/pii/S0306261920306255> (visited on 08/24/2023).